National Conference with International Participation
ENGINEERING MECHANICS 2007
Svratka, Czech Republic, May 14 – 17, 2007

TOWARDS MICROSTRUCTURE-BASED RANDOM FIELD MODELS OF HETEROGENEOUS MEDIA

M. Lombardo*, J. Zeman*, G. Falsone*

Summary: *In this contribution, we present and mutually compare three approaches to the analysis of finite heterogeneous elastic bodies with a random arrangement of individual phases. The examined methods are the representatives of perturbation techniques, non-perturbative approaches and the tools of the mechanics of composite materials, respectively. The emphasis is put on a rational construction of the underlying random fields using the spatial statistics related to the material in question. Advantages and limitations of the methods are illustrated on the elastic analysis of an irregular masonry panel.*

1. Introduction

Almost every material displays a non-homogeneous structure at a sufficient level of resolution and this heterogeneity governs the mechanical response of the analyzed structure. Even though the theory of heterogeneous media has experienced a significant development in the recent decades, the analysis and numerical simulations have mainly been based on an assumption of the scale separation. Under this hypothesis, behavior of the body can be treated separately on (at least) two well-separated lengthscales, the first one corresponding to the macroscopic response, and the second one describing the response of a representative sample of the heterogeneous material. This assumption, although acceptable for a variety of material systems a loading programs, become too restrictive when addressing e.g. systems with an intermediate gap between the relevant scales or for the cases where the scale jump decreases as the effect of loading (such as in the failure analyses in heterogeneous media).

The abovementioned limitations can be overcome when describing the heterogeneous body via a random field with spatially varying properties. Not only that such a description is physically more correct and free of the separation-of-scale assumption, but is also allows exploiting the machinery of stochastic mechanics to arrive at the statistics of the quantity of interest. Moreover, under assumption of well-separated lengthscales, the stochastic description splits into independent analyses on the macro- and micro-scales, e.g. (Jikov at el., 1994; Torquato, 2002). The major difficulty of the methodology is, however, the fact that in the computational treatment, the random field is introduced without a clear link with the underlying material and its microstructure.

* Mariateresa Lombardo, Giovanni Falsone, Dipartimento di Ingegneria Civile (DIC), Università di Messina, Salita Sperone 31, 98166, S.Agata-MESSINA, Italy, e-mail: mlombardo@ingegneria.unime.it, gfalsone@ingegneria.unime.it, Jan Zeman, Faculty of Civil Engineering, Czech Technical University in Prague, 166 29 Prague 6, e-mail: zemanj@cml.fsv.cvut.cz

In this paper, we present an attempt to propose a framework for a rational construction of a random field tied to the heterogeneous material in question. To this end, the potential provided by the qualitative method of microstructure description is exploited in Section 2 to arrive at the first- and second-order statistics of the random field. With such information in hand, three different approaches to the determination of the statistics of a finite body with a finite microstructure are examined. In particular, the improved perturbation method is introduced first in Section 3, followed by a more refined Karhunen-Loeve series representation briefly discussed in Section 4. Section 5 deals with a method originating from the techniques developed in the mechanics of composite media. The selected methods are mutually compared in Section 6. Finally, Section 7 introduces possible extensions and refinements of the studied approaches.

2. Quantification of microstructure morphology and random field statistics

Consider a sample θ of a two-phase random medium. A basic description of its microstructure is given in terms of the so-called characteristic function

$$\chi_s(\mathbf{x},\theta) = \begin{cases} 1 \Leftrightarrow \mathbf{x} \in \Omega_s(\theta) \\ 0 \Leftrightarrow \mathbf{x} \in \Omega_m(\theta) \end{cases} \tag{1}$$

where Ω_s and Ω_m are the portion of the sample body Ω occupied by phase s and m, respectively. Using this function, the stiffness tensor at any point of Ω can be expressed as

$$\mathbf{C}(\mathbf{x}) = \chi_s(\mathbf{x},\theta)\mathbf{C}_s + \left(1-\chi_s(\mathbf{x},\theta)\right)\mathbf{C}_m \tag{2}$$

where $\mathbf{C}_s$ and $\mathbf{C}_m$ are the deterministic stiffness matrices of the two constituents.

In the field of composite materials the characteristic function has to be statistically defined through the knowledge of the so-called *n*-point correlation function. These functions give a measure of the probability of finding *n* points all lying in the region of the domain occupied by one of the constituent materials. If we limit our attention to functions of the order one and two, a description of a random medium will be provided by

$$\mathrm{S}_s^{(1)}(\mathbf{x}) = \mathrm{P}\left(\chi_s(\mathbf{x},\theta) = 1\right) \tag{3}$$

$$\mathrm{S}_s^{(2)}\left(\mathbf{x}_1,\mathbf{x}_2\right) = \mathrm{P}\left(\chi_s\left(\mathbf{x}_1,\theta\right)\chi_s\left(\mathbf{x}_2,\theta\right) = 1\right) \tag{4}$$

The one-point probability function in Eq. (3) gives the probability of finding the phase *s* at $\mathbf{x}$ and the two-point probability function in Eq.(4) denotes the probability of finding simultaneously the phase *r* at $\mathbf{x}_1$ and the phase *s* at $\mathbf{x}_2$.

If the ergodicity assumption is made, the function $\chi_s(\mathbf{x},\theta)$ can be considered as a random field whose statistical moments coincide with the corresponding *n*-point correlation functions. The first two moments are

$$\mathrm{E}\left[\chi_s(\mathbf{x})\right] \equiv \mathrm{S}_s^{(1)}(\mathbf{x}) \tag{5}$$

$$\mathrm{E}\left[\chi_s(\mathbf{x}_1)\chi_s(\mathbf{x}_2)\right] \equiv \mathrm{S}_s^{(2)}(\mathbf{x}_1,\mathbf{x}_2) \tag{6}$$

If the heterogeneous material can be described by a statistically homogeneous field, then moments of $\chi_s(\mathbf{x})$ do not depend on the absolute position of the points but on the relative one: $(\mathbf{x}_2-\mathbf{x}_1)$. This implies that the mean $\mathrm{E}\left[\chi_s(\mathbf{x})\right]$ is constant for any point, while the second order moment is

$$\mathrm{E}\left[\chi_s(\mathbf{x}_1)\chi_s(\mathbf{x}_2)\right] \equiv \mathrm{S}_s^{(2)}(\mathbf{x}_2-\mathbf{x}_1) \tag{7}$$

It is not difficult to verify that the *n*-th moments at a single point have the following form

$$\mathrm{E}\left[\chi_s^n(\mathbf{x})\right]=\gamma_s \qquad \forall n \tag{8}$$

Eqs.(7) and (8) imply that the second order correlation function of the field $\chi_s(\mathbf{x})$ is given by

$$\mathrm{R}_{\chi_s}^{(2)}(\mathbf{x}_2-\mathbf{x}_1)=\mathrm{S}_s^{(2)}(\mathbf{x}_2-\mathbf{x}_1)-\gamma_s^2 \tag{9}$$

while the variance is

$$\sigma_{\chi_s}^2=\mathrm{E}\left[\chi_s^2\right]-\mathrm{E}\left[\chi_s\right]^2=\gamma_s-\gamma_s^2 \tag{10}$$

The statistical descriptors for a real microstructure can be evaluated on the basis of a digitized micrograph of the sample in binary format. A digital representation can be considered as a discretization of the characteristic function $\chi_s(\mathbf{x})$ in terms of a $N_{x_1}\times N_{x_2}$ bitmap. Replacing the point coordinates (x_1,x_2) by the pixel (i,j) located in *i*-th row and *j*-th column of the bitmap the characteristic function is defined by the discrete value $\chi_s(i,j)$. The one-point and two-point correlation functions, under the periodic boundary condition (Gajdošík et al., 2006), may be estimated by using the following relations

$$\mathrm{S}_s^{(1)}=\frac{1}{N_{x_1}N_{x_2}}\sum_{i=1}^{N_{x1}}\sum_{j=1}^{N_{x2}}\chi_s(i,j)=\gamma_s \tag{11}$$

$$\mathrm{S}_s^{(2)}(m,n)=N_{x1}N_{x2}\sum_{i=1}^{N_{x1}}\sum_{j=1}^{N_{x2}}\chi_s(i,j)\chi_s\left(1+(i+m)\%N_{x_1},1+(j+n)\%N_{x_2}\right) \tag{12}$$

where *m* and *n* assume here the significance of pixel distance between two generic points and % denotes modulo. To automate the acquisition of these functions, software working in Matlab was implemented (Falsone & Lombardo, 2006). First step deals with generation of a binary image starting from a digital color image of masonry, giving as results the values of γ_s and $\mathrm{S}_s^{(2)}(m,n)$. In Figure 1, the results obtained by STONES for an irregular masonry panel that will be treated in the analysis part are reported.

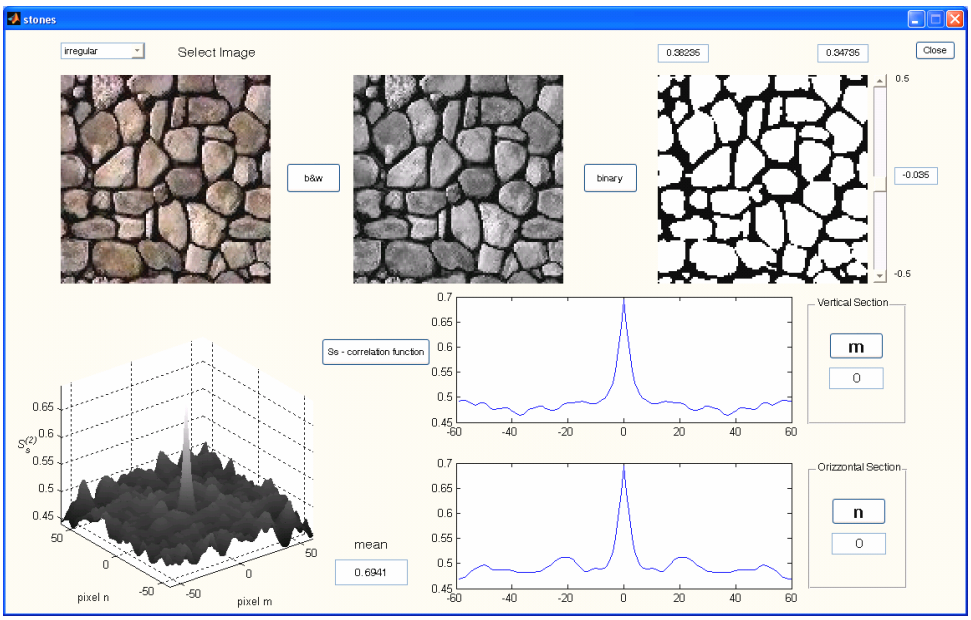

Figure 1. Example of graphical user interface of STONES for chaotic masonry panel.

Once that the stochastic field $\chi_s(\mathbf{x})$ is known through its correlation functions, the corresponding statistics of the elastic moduli $C_{ij}(\mathbf{x})$ can be obtained starting from Eq.(2). In particular the mean and the second order correlation are given by

$$\mathrm{E}\left[C_{ij}(\mathbf{x})\right] = \gamma_s C_{ij}^{(s)} + (1-\gamma_s) C_{ij}^{(m)} \tag{13}$$

$$\mathrm{R}_{C_{ij}C_{kl}}^{(2)}(\mathbf{x}_2-\mathbf{x}_1) = \mathrm{R}_{\chi_s}^{(2)}(\mathbf{x}_2-\mathbf{x}_1)\times\left(C_{ij}^{(s)}-C_{ij}^{(m)}\right)\left(C_{kl}^{(s)}-C_{kl}^{(m)}\right) \tag{14}$$

The auto-correlation function of the component C_{ij} of the stiffness matrix can be obtained by setting $i \equiv k$, $j \equiv l$ in Eq.(14), that is

$$\mathrm{R}_{C_{ij}C_{kl}}^{(2)}(\mathbf{x}_2-\mathbf{x}_1) = \mathrm{R}_{\chi_s}^{(2)}(\mathbf{x}_2-\mathbf{x}_1)\times\left(C_{ij}^{(s)}-C_{ij}^{(m)}\right)^2 \tag{15}$$

and the variance is

$$\sigma_{C_{ij}}^2 = \sigma_{\chi_s}^2\left(C_{ij}^{(s)}-C_{ij}^{(m)}\right)^2 = \left(\gamma_s-\gamma_s^2\right)\left(C_{ij}^{(s)}-C_{ij}^{(m)}\right)^2 \tag{16}$$

The reported relation evidence that the stochastic characterization up to second order of the stiffness matrix require the knowledge of γ_s and $\mathrm{S}_s^{(2)}(\mathbf{x}_2-\mathbf{x}_1)$, besides of the elements of $\mathbf{C}_s$ and $\mathbf{C}_m$.

It is clear from Eq.(1) that the indicator function $\chi_s(\mathbf{x})$ is a discrete random field with a continuous parameter in the spatial domain, and the random field $\mathbf{C}(\mathbf{x})$ is also discrete with a continuous parameter, as can be shown in Figure 2 in terms of a mono-dimensional problem (Ostoja-Starzewski, 1998).

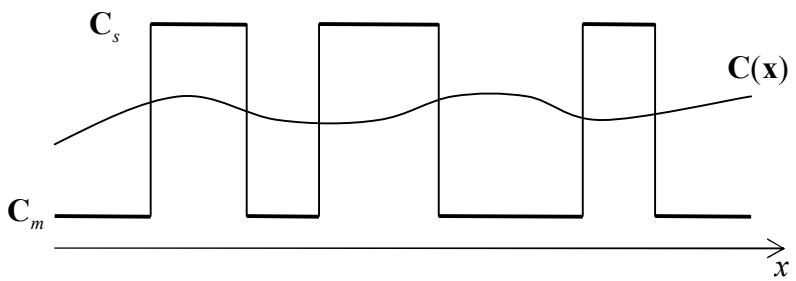

Figure 2. From a piecewise-constant realization of a composite to a continuum random field

3. Stochastic Finite Element Method - Perturbative approaches

Using the standard finite element formulation, a static analysis requires the solution of the following system of equations

$$\mathbf{K}(\chi_s)\mathbf{u}(\chi_s) = \mathbf{F} \tag{17}$$

where the load vector $\mathbf{F}$ is assumed to be deterministic and the global stiffness matrix $\mathbf{K}$ is stochastic due to randomness in the material properties. Because the global stiffness matrix $\mathbf{K}$ is stochastic, the displacement vector $\mathbf{u}$ is also stochastic. In particular $\mathbf{K}$ and $\mathbf{u}$ depend on the random field $\chi_s(\mathbf{x})$.

The solution of equation (17) requires a representation of the stochastic field in terms of discrete random variables. Their statistical properties are related on the chosen finite element

mesh and the discretization of the random field is required to define the "best" approximation. Two different considerations control the size of an element (Matthies et al., 1997). The first way is usually used in deterministic finite elements and the design of the mesh is governed by expected stress gradient and geometry. The second is linked with the correlation length describing the rate of fluctuation of the random field. The distance between two adjacent random variables therefore has to be short enough to capture the essential features of the random field. An element size of half of the correlation length suffices for a satisfactory representation of the stochastic field.

The discretization of the random field can be done by using one of the literature methods, among which the most simple (even if not the most accurate) is the midpoint method. Usually the value at the center of the element is used to represent the stochastic field. If $\alpha^{(e)}$ is the value of $\chi_s(\mathbf{x})$ at the finite element centroid, the elastic modulus matrix is constant inside it, with value

$$\mathbf{C}^{(e)}(x_1, x_2) = \mathbf{C}_m + \left(\mathbf{C}_s - \mathbf{C}_m\right)\alpha^{(e)} = \mathbf{C}^{(e)}\left(\alpha^{(e)}\right) \tag{18}$$

The element stiffness matrix is calculated from standard finite element methodology and is expressed as

$$\mathbf{K}^{(e)}\left(\alpha^{(e)}\right) = \int_{A^{(e)}} \mathbf{B}^{\mathrm{T}}(\mathbf{x})\mathbf{C}^{(e)}\left(\alpha^{(e)}\right)\mathbf{B}(\mathbf{x})\,dA \tag{19}$$

where $\mathbf{B}(\mathbf{x})$ is the deterministic strain-displacement matrix. After assembling all element stiffness matrix in the global stiffness matrix, the solving equation becomes

$$\mathbf{K}(\boldsymbol{\alpha})\mathbf{u}(\boldsymbol{\alpha}) = \mathbf{F} \tag{20}$$

$\boldsymbol{\alpha}$ being the vector collecting the set of random variables.
Solving Eq.(20) via SFE method means to find the probabilistic information on the derived random variables $\mathbf{u}(\boldsymbol{\alpha})$, once that the characteristic of random variables $\boldsymbol{\alpha}$ are given. In our application these last are obtained as mentioned in Section 2.

There are various approaches to formulating an SFE method to obtain the statistics of global displacement vector $\mathbf{u}$. In this work, an improved perturbation technique by Elishakoff et al. (1995) is used. It takes into account mean and correlation information on uncertain parameters in computing the mathematical expectation of the response; then, the improved expectation is used to calculate covariance of the response. Following this approach the mean of the response is given by

$$\mathrm{E}[\mathbf{u}] = \mathbf{A}^{-1}\mathbf{F} \tag{21}$$

where

$$\mathbf{A} = \mathbf{K}_0 - \sum_{i=1}^{N}\sum_{j=1}^{N}\mathbf{K}_i'\left(\mathbf{K}_0\right)^{-1}\mathbf{K}_j' E\left[\alpha_i \alpha_j\right] \tag{22}$$

and the covariance matrix of displacements is

$$\boldsymbol{\Sigma}_{\mathbf{u}(\boldsymbol{\alpha})} = \mathbf{K}_0^{-1}\mathbf{C}\,\mathbf{K}_0^{-1} \tag{23}$$

where

$$\mathbf{C} = \sum_{i=1}^{N}\sum_{j=1}^{N}\mathbf{K}_i'\ \mathrm{E}[\mathbf{u}]\mathrm{E}[\mathbf{u}]^T\ \mathbf{K}_j' E\left[\alpha_i \alpha_j\right] \tag{24}$$

It can be observed that the stiffness matrix $\mathbf{A}$ differs from $\mathbf{K}_0$ and the mean value of the response depends on the second-order moment of uncertain parameters.

4. Karhunen-Loève expansion

Series expansion methods, used for unknown random material parameters, have provided an attractive alternative for the problems involving random fields with large variation. Zhang & Ellingwood (1994) showed that any orthogonal expansion of a random field can be related to the Karhunen-Loève expansion of that random field.

The Karhunen-Loève expansion (KL-expansion) for a random field $H(\mathbf{x},\theta)$, function of the position vector $\mathbf{x}$ defined over the domain D and with θ belonging to the space of random events Ω, has the form:

$$H(\mathbf{x},\theta) = \mu + \sum_{i=1}^{\infty} \sqrt{\lambda_i}\,\xi_i(\theta) f_i(\mathbf{x}) \tag{25}$$

where μ is the mean of the field, λ_i and $f_i(\mathbf{x})$ are the eigenvalues and eigenfunctions (decreasing in magnitude) of the covariance function $\Sigma_H(\mathbf{x}_1,\mathbf{x}_2)$, $\xi_i(\theta)$ is a set of random variables (Sudret & Der Kiureghian, 2000).

The KL-expansion is based on the spectral expansion of covariance function $\Sigma_H(\mathbf{x}_1,\mathbf{x}_2)$ of the field, where $\mathbf{x}_1$ and $\mathbf{x}_2$ are two spatial coordinates. Its use is limited as the covariance function is not known *a priori*, therefore it provides a powerful means for representing *input* random field when the covariance structure is known. Since the covariance function $\Sigma_H(\mathbf{x}_1,\mathbf{x}_2)$ is bounded, symmetric and positive, it has all eigenfunctions mutually orthogonal and they form a complete set spanning the function space to which $H(\mathbf{x},\theta)$ belongs. It can be decomposed into

$$\Sigma_H(\mathbf{x}) = \sum_{i=1}^{\infty} \lambda_i f_i(\mathbf{x}_1) f_i(\mathbf{x}_2) \tag{26}$$

and eigenfunctions $f_i(\mathbf{x})$ satisfying the equation

$$\int_D f_i(\mathbf{x}) f_j(\mathbf{x})\, d\mathbf{x} = \delta_{ij} \tag{27}$$

Eigenvalues λ_i and eigenfunctions $f_i(\mathbf{x})$ of covariance can be founded solving the homogeneous Fredholm integral equation of the second kind

$$\int_D \Sigma_H(\mathbf{x}_1,\mathbf{x}_2) f_i(\mathbf{x}_2)\, d\mathbf{x}_2 = \lambda_i f_i(\mathbf{x}_1) \tag{28}$$

The parameter $\xi_i(\theta)$ in Eq.(25) is a set of uncorrelated standardized random variables which can be expressed as

$$\xi_i(\theta) = \frac{1}{\sqrt{\lambda_i}} \int_D \left[H(\mathbf{x},\theta) - \mu(\mathbf{x}) \right] f_i(\mathbf{x})\, d\mathbf{x} \tag{29}$$

with mean and covariance function given by

$$E\left[\xi_i(\theta)\right] = 0, \quad E\left[\xi_i(\theta)\xi_j(\theta)\right] = 0 \tag{30}$$

The most important aspect of the representation (25) is that the spatial random fluctuation has been decomposed into a set of deterministic function in the spatial variables multiplyng random coefficient that are independent from these variables.

For practical implementation, the series is approximated by a finite numbers of terms M:

$$\hat{H}(\mathbf{x},\theta) = \mu + \sum_{i=1}^{M} \sqrt{\lambda_i}\,\xi_i(\theta) f_i(\mathbf{x}) \tag{31}$$

and the corresponding approximate covariance function is

$$\hat{\Sigma}_H(\mathbf{x}) = \sum_{i=1}^{M} \lambda_i f_i(\mathbf{x}_1) f_i(\mathbf{x}_2) \tag{32}$$

Ghanem & Spanos (1991a) have shown this truncated series to be optimal; the covariance eigenfunctions basis $f_i(\mathbf{x})$ is optimal in the sense that the mean square error (integrated over D) resulting from a truncation after M-th terms is minimized (with respect to the value it would take when any complete basis $f_i(\mathbf{x})$ is chosen).

If $H(\mathbf{x},\theta)$ is a Gaussian random field, each random variable $\xi_i(\theta)$ is Gaussian, then a vector of zero-mean uncorrelated Gaussian random variables is an appropriate choice of $\xi_i(\theta)$. The latter can be generated by available subroutines and then multiplied by the eigenfunctions and eigenvalues derived from the solution of Eq.(28).

The efficiency of KL-expansion for simulating random fields hinges crucially on the availability of accurate eigenvalues and eigenfunctions of the covariance function by solving the Fredholm equation. Eq.(28) can be solved analytically only for few autocovariance function and geometries of D. Detailed closed form solutions for some covariance kernels of one-dimensional homogeneous field can be found in Ghanem & Spanos (1991b).

Extension to two-dimensional fields defined for similar correlation functions on a rectangular domain can be obtained by product of one-dimensional solution, e.g.

$$\lambda_n = \lambda_i^{(1)} \cdot \lambda_j^{(2)} \tag{33}$$

$$f_n(\mathbf{x}) = f_n(x_1, x_2) = f_i^{(1)}(x_1) f_j^{(2)}(x_2) \tag{34}$$

where the superscript (1) and (2) define two orthogonal direction.

However, for most covariance functions, numerical methods are required. In this paper, the Galerkin method is used (Phoon et al., 2002). Each eigenfunctions $f_i(\mathbf{x})$ is approximated by a linear combination of chosen basis functions and setting that the error in Eq.(28) to be orthogonal to each basis function is obtained a finite order system of linear algebraic equation.

A careful convergence study of the truncated KL-expansion (Huang et al., 2001) showed the dependence of the number of terms in series expansion from the ratio of domain length L to the correlation parameter b. The number of terms M in series expansion must be selected to produce reasonably accurate simulation of the random field. For weakly correlated process (large L/b) a large value of M is needed. It can be seen that the magnitude of each eigenvalue λ_i increases with the domain length. Hence, the decay to zero of eigenvalues is slower and a larger number of terms are required to represent the field. To illustrate this phenomena, Figure 3 shows decay in eigenvalues with index *i*. In Figure 4 are plotted four eigenfunctions obtained for a two dimensional domain using Galerkin method to solve the Fredholm integral equation (28).

The KL-expansion (Eq.(32)) is used to generate sample function of the input random field. To evaluate the statistics of the response, for the finite element problem, Monte Carlo Simulation (MCS) is performed. Realizations of elastic modulus of the square plate under

analysis are numerically simulated using the KL-expansion method. For each of the realization, the deterministic problem is solved and the statistics are obtained.

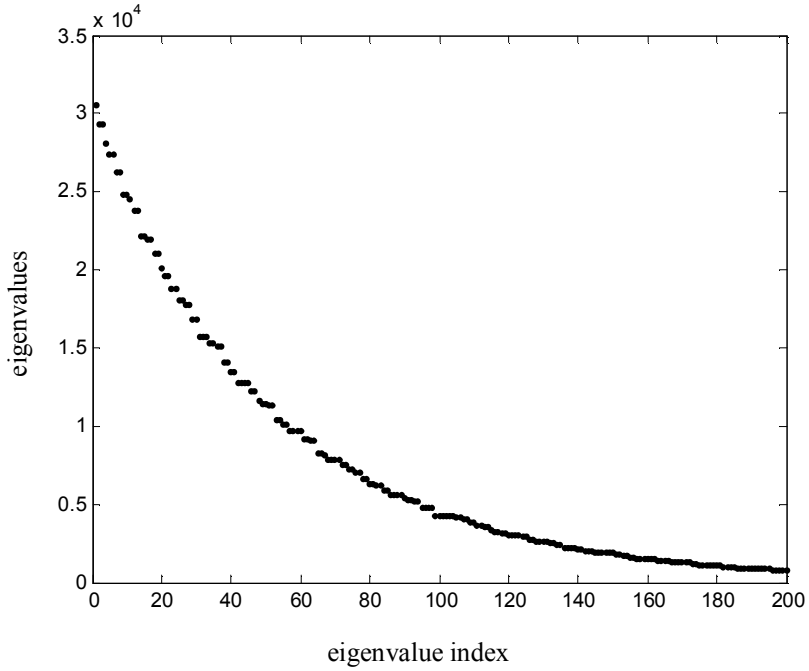

Figure 3. Eigenvalues decaying with eigenvalue index *i* for square exponential

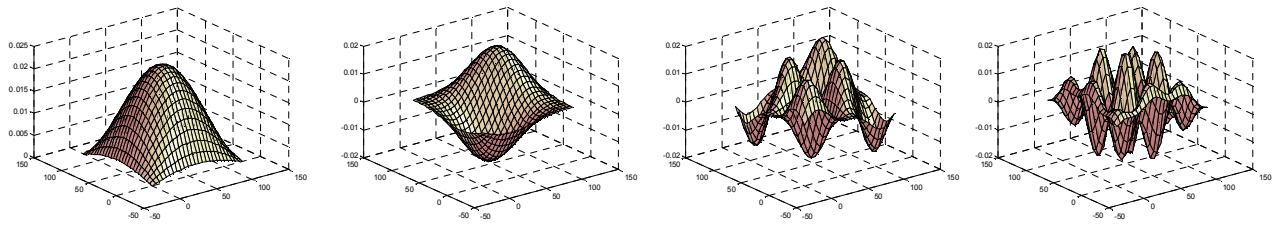

Figure 4. Eigenfunctions 1,2,12,24.

The numerical application showed in Section 6, is performed using the Gaussian random field hypothesis for elastic modulus. The C.O.V.=0.3 (coefficient of variation of the mean) was selected and its value realistically reproduce the physically variability in elastic properties of the random medium sample. For greater value of C.O.V. chosen, negative values of Young's modulus acquire considerable probability, whereas the material properties are positive in nature and non physical result could be included in the simulation.

It should be emphasized that the assumption of Gaussian constitutive tensor is questionable, particularly for strongly non-Gaussian media, e.g. bimodal cases corresponding to bi-phase composites. For these physical random materials it would be appropriate to use Lognormal or Beta probability density. The working assumption of the authors is the Gaussian hypothesis which was made in a number of previous works.

Unbiased estimates of the mean and variance of a given statistical sample are given by

$$E^{MC}\left[\mathbf{u}\right]=\frac{1}{N_{sim}}\sum_{i=1}^{N_{sim}}\mathbf{u}\left(\theta_i\right) \tag{35}$$

$$Var^{MC}\left[\mathbf{u}\right]=\frac{1}{N_{sim}-1}\sum_{i=1}^{N_{sim}}\left[\mathbf{u}^2\left(\theta_i\right)-N_{sim}\left(E^{MC}\left[\mathbf{u}\right]\right)^2\right] \tag{36}$$

where N_{sim} is the number of samples considered, $\mathbf{u}\left(\theta_i\right)$ is the nodal displacement vector associated with sample θ_i, and $\mathbf{u}^2\left(\theta_i\right)$ is the vector containing the square values of nodal displacements.

5. Hashin-Strikman variational approach

The last approach builds on the classical principles of the variational principles for the heterogeneous media. The basic principle of the method is the introduction of a reference homogeneous body characterized a stiffness tensor $\boldsymbol{C}_0$. For any realization θ of the media, the heterogeneity of the material is accounted for using the polarization stress $\boldsymbol{\tau}(\boldsymbol{x};\theta)$:

$$\boldsymbol{\sigma}\left(\boldsymbol{x};\theta\right)=\boldsymbol{C}\left(\boldsymbol{x};\theta\right):\boldsymbol{\varepsilon}\left(\boldsymbol{x};\theta\right)=\boldsymbol{C}_0\boldsymbol{\varepsilon}\left(\boldsymbol{x};\theta\right)+\boldsymbol{\tau}\left(\boldsymbol{x};\theta\right), \tag{37}$$

where $\boldsymbol{\sigma}$ and $\boldsymbol{\varepsilon}$ denote the stress and strain field in the composite, respectively. The additional unknown follows from the stationarity conditions of the associated Hashin-Shtrikman functional

$$\left(\boldsymbol{u}\left(\boldsymbol{x};\theta\right),\boldsymbol{\tau}\left(\boldsymbol{x};\theta\right)\right)=\arg\operatorname{stat}\left\{\begin{array}{l}\dfrac{1}{2}\displaystyle\int_D\boldsymbol{\varepsilon}\left(\boldsymbol{v}\left(\boldsymbol{x}\right)\right):\boldsymbol{C}_0:\boldsymbol{\varepsilon}\left(\boldsymbol{v}\left(\boldsymbol{x}\right)\right)+\boldsymbol{\omega}\left(\boldsymbol{x};\theta\right):\left[\boldsymbol{C}\left(\boldsymbol{x};\theta\right)-\boldsymbol{C}_0\right]^{-1}:\boldsymbol{\omega}\left(\boldsymbol{x};\theta\right)\mathrm{d}\boldsymbol{x}\\ -\displaystyle\int_D\boldsymbol{v}\left(\boldsymbol{x}\right)\cdot\boldsymbol{f}\left(\boldsymbol{x}\right)\mathrm{d}\boldsymbol{x}-\int_{\Gamma_t}\boldsymbol{v}\left(\boldsymbol{x}\right)\cdot\boldsymbol{t}\left(\boldsymbol{x}\right)\mathrm{d}\boldsymbol{x}\,\Big|\,\boldsymbol{v}\left(\boldsymbol{x}\right),\boldsymbol{\omega}\left(\boldsymbol{x};\theta\right)\end{array}\right\}$$

where $\boldsymbol{v}(\boldsymbol{x})$ denote the trial kinematically admissible displacement field, $\boldsymbol{\omega}(\boldsymbol{x};\theta)$ is a realization-dependent polarization field; $\boldsymbol{f}(\boldsymbol{x})$ and $\boldsymbol{t}(\boldsymbol{x})$ are the body forces and boundary tractions, respectively (Luciano & Willis, 2006).

When searching for the statistics of the overall response, the critical point of the previous relation are to be sought simultaneously for all the realization of the material weighted by the probability of occurrence $p(\theta)$. To this end, the searched displacement field is decomposed into two parts and the polarization field is expanded in the form:

$$\boldsymbol{u}\left(\boldsymbol{x};\theta\right)=\boldsymbol{u}_0\left(\boldsymbol{x}\right)+\boldsymbol{u}_1\left(\boldsymbol{x};\theta\right),\quad\boldsymbol{\tau}\left(\boldsymbol{x};\theta\right)\approx\chi_s\left(\boldsymbol{x};\theta\right)\boldsymbol{\tau}_s\left(\boldsymbol{x}\right)+\left(1-\chi_s\left(\boldsymbol{x};\theta\right)\right)\boldsymbol{\tau}_m\left(\boldsymbol{x}\right) \tag{38}$$

with the $\boldsymbol{u}_0$ denoting the part corresponding to the loading effects, $\boldsymbol{u}_1$ expressing the effects of heterogeneity; $\boldsymbol{\tau}_s$ and $\boldsymbol{\tau}_m$ store the polarization fields related to individual phases. When performing the optimization for the kinematics first, the optimality conditions for the polarization fields attain the form ($r,j = s,m$):

$$\begin{aligned}&\int_D\gamma_r\left(\boldsymbol{x}\right)\boldsymbol{\theta}_r\left(\boldsymbol{x}\right):\left[\boldsymbol{C}_r-\boldsymbol{C}_0\right]^{-1}:\boldsymbol{\tau}_r\left(\boldsymbol{x}\right)\mathrm{d}\boldsymbol{x}+\sum_j\int_D\boldsymbol{\theta}_r\left(\boldsymbol{x}\right):\int_D S^{(2)}_{rj}\left(\boldsymbol{x},\boldsymbol{y}\right)\boldsymbol{\Gamma}_0\left(\boldsymbol{x},\boldsymbol{y}\right):\tau_j\left(\boldsymbol{y}\right)\mathrm{d}\boldsymbol{x}\mathrm{d}\boldsymbol{y}=\\&\int_D\gamma_r\left(\boldsymbol{x}\right)\boldsymbol{\theta}_r\left(\boldsymbol{x}\right):\boldsymbol{\varepsilon}_0(x)\mathrm{d}\boldsymbol{x}\end{aligned} \tag{39}$$

where $\boldsymbol{\Gamma}_0$ denotes the function related to the Green's function of the homogeneous body with homogeneous boundary data (Luciano & Willis, 2006) and $\boldsymbol{\varepsilon}_0$ is the strain field in the reference structure.

Searching for an approximate solution requires the introduction of a set of basis function for the polarization stresses and the action of the function $\boldsymbol{\Gamma}_0$. In the framework of the finite element method, the function can be approximated via ($\boldsymbol{K}_0$ is the reference stiffness matrix)

$$\boldsymbol{\Gamma}_0\left(\boldsymbol{x},\boldsymbol{y}\right)\approx\boldsymbol{\Gamma}_0^h\left(\boldsymbol{x},\boldsymbol{y}\right)=\boldsymbol{B}\left(\boldsymbol{x}\right)\left[\boldsymbol{K}_0\right]^{-1}\boldsymbol{B}^{\mathrm{T}}\left(\boldsymbol{y}\right) \tag{40}$$

and Eq. (39) reduces to the system of linear equations

$$\boldsymbol{K}_r \boldsymbol{d}_r + \sum_j \boldsymbol{K}_{rj} \boldsymbol{d}_j = \boldsymbol{R}_r \tag{41}$$

with the individual terms given by

$$\begin{aligned} \boldsymbol{K}_r &= \int_D \gamma_r(\boldsymbol{x}) \boldsymbol{N}(\boldsymbol{x}) : \left[\boldsymbol{C}_r - \boldsymbol{C}_0\right]^{-1} : \boldsymbol{N}(\boldsymbol{x}) \mathrm{d}\boldsymbol{x} \\ \boldsymbol{K}_{rj} &= \int_D \boldsymbol{N}(\boldsymbol{x}) : \int_D S_{rj}^{(2)}(\boldsymbol{x}, \boldsymbol{y}) \boldsymbol{\Gamma}_0^h(\boldsymbol{x}, \boldsymbol{y}) : \boldsymbol{N}(\boldsymbol{y}) \mathrm{d}\boldsymbol{x} \mathrm{d}\boldsymbol{y} \\ \boldsymbol{R}_r &= \int_D \gamma_r(\boldsymbol{x}) \boldsymbol{\theta}_r(\boldsymbol{x}) : \boldsymbol{\varepsilon}_0^h(x) \mathrm{d}\boldsymbol{x} \end{aligned} \tag{42}$$

where $\boldsymbol{N}(\boldsymbol{x})$ denote the basis functions used to approximate the sought polarization field. Once the approximation of the polarization field is available, the statistics of the response can be evaluated by post-processing steps introduced in (Luciano & Willis, 2006).

6. Numerical example

In this section, we examine the numerical results obtained from an elastic analysis made on the masonry sample shown below. A finite element model was constructed for the panel under plane stress, loaded by uniform pressure in vertical direction and by self-weight, shown in Figure 5. The two-dimensional domain is a square uniformly discretized into 24×24 square elements.

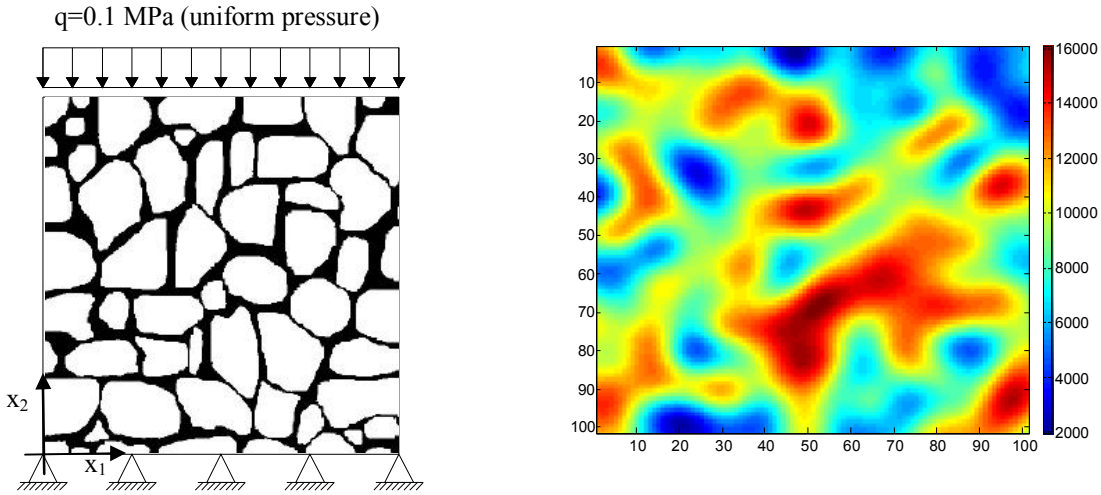

(a) (b)

Figure 5. Numerical example. (a) Geometry and loading, (b) Typical realization of Gaussian field

The FE considered in this analysis is the isoparametric four-node quadrilateral element with 8 DOF (horizontal and vertical displacements). The stochastic 2D field of the corresponding indicator function $\chi_s(\mathbf{x})$ is characterized by the statistic descriptors obtained by STONES as showed in Figure 1. In the context of perturbation approach, the mid-point method is adopted to discretize the random field. It must be noticed that the spatial mesh is assumed equal to the discretization of the random field, with attention at the general rules described in Section 3. The results obtained by first-order perturbation method and improved

method have been compared with those obtained via Karhunen-Loève model coupled with the Monte Carlo integration. The Hashin-Shtrikman approach is currently in the development.

For simplicity, Young's modulus is described by a Gaussian random field and its statistical information is directly obtained through the micromechanical description. The more appropriate analytical expression of correlation is the square exponential function; if we assume the isotropic hypothesis in the constitutive law, the correlation function has the form

$$\rho\left(d_1, d_2\right) = \exp\left(-\frac{d_1^2 + d_2^2}{b^2}\right) \tag{43}$$

where d_1 and d_2 are separation distance, and b is the parameter describing the correlation length. A sample of the Gaussian elastic modulus field generated using KL-expansion (31) is shown in Figure 5b.

Mean and standard deviation for nodal displacements were computed by Eqs. (35) and (36) with the number of realization in MCS set to 1000. In Figure 6 the mean values of nodal vertical displacements in the top of the panel are shown and the values of the mean displacements augmented and diminished by their standard deviation values are plotted with the dotted line. Moreover, the results of the first-order perturbation method (e.g. (Sudret & Der Kiureghian, 2000) are presented for a comparison.

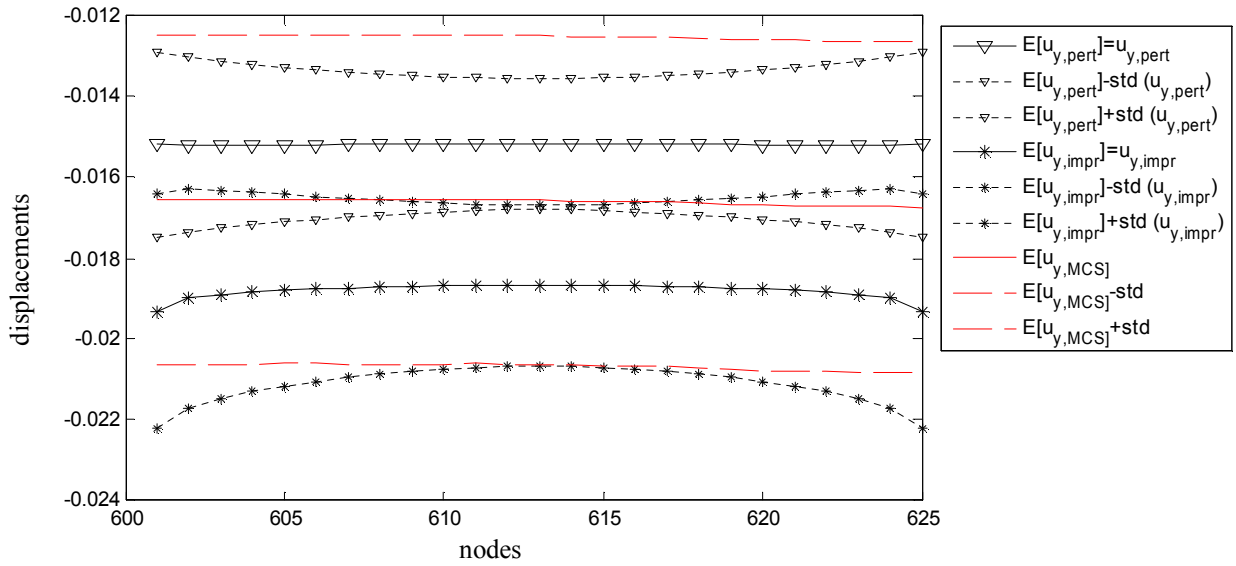

Figure 7. Nodal displacements and standard deviation on the top of the square panel

7. Conclusions and future work

In this contribution, the first numerical results of microstructure-based random field simulations are presented. The numerical results obtained for a finite-size elastic panel allow us to reach the following conclusions:

i) The elements of quantification of random spatial statistics can be efficiently used to construct the first- and second-order statistics of stationary random fields including the anisotropy effects.

ii) When compared with the classical method, the improved perturbation technique leads to narrower estimates of the overall response of the system. Moreover, the method utilizes more details of the available statistical data.

iii) The Karhunen-Loève series representation provides an interesting alternative to the perturbation-based method, in particular from the point of view of computational

efficiency. Nevertheless, the response predicted by the method shows a certain deviation from the perturbative approaches.

iv) The Hashin-Shtrikman approach takes advantage of the specific form of the random field and therefore, it can be used as the reference solution.

v) In overall, the Karhunen-Loève representation seems to be the most attractive method for the extension to the non-linear regime. However, before taking this step, a robust non-Gaussian variant of the method is needed.

Acknowledgements. The financial support of this work was provided by project of the Grant Agency of the Czech Republic No. 106/07/1244.

8. References

Elishakoff I. & Ren Y.J.(1995), Improved finite element method for stochastic problems, *Chaos, Solitons & Fractals*, 5, 5, pp.833-846.

Falsone G. & Lombardo M. (2006), About the stochastic representation of the mechanical properties of irregular masonry panels, *Proc. Computational Stochastic Mechanics 5*, Rhodos (Greece), In Press.

Gajdošík J., Zeman J. & Šejnoha M., (2006), Qualitative analysis of fiber composite microstructure: Influence of boundary condition, *Probabilistic Engineering Mechanics*, 21, 4, pp. 317-329.

Ghanem R. G. & Spanos P.D. (1991a) *Stochastic finite - elements – A spectral approach.* Springer Verlag.

Ghanem R. G. & Spanos P.D. (1991b) Spectral stochastic finite - element formulation for reliability analysis. *Journal of Engineering Mechanics*, 117, 10, pp.2351-2372.

Huang S.P., Quek S.T &. Phoon K.K. (2001), Convergence study of truncated Karhunen-Loève expansion for simulation of stochastic process, *International Journal for Numerical Methods in Engineering*, 52, pp. 1029-1043.

Jikov, V.V. & Kozlov, S.M. & Oleinik, OA (1994) *Homogenization of differential operators and integral functionals.* Springer Verlag.

Luciano R. & Willis, J. R. (2006) Hashin–Shtrikman based FE analysis of the elastic behaviour of finite random composite bodies, *International Journal of Fracture*, 137, 1—4, pp. 261—273.

Matthies H.G., Brenner C.E., Bucher C.G.& Soares C. (1997), Uncertainties in probabilistic numerical analysis of structures and solids – Stochastic finite elements, *Structural Safety*, 19, 3, pp.283-336.

Ostoja-Starzewski M. (1998), Random fields models of heterogeneous materials, *International Journal of Solids and Structures*, 35, 2, pp.2429-2455.

Phoon K.K., Huang S.P. & Quek S.T., Implementation of Karhunen-Loève expansion for simulation using a wavelet-Galerkin scheme, *Probabilistic Engineering Mechanics*, 17, 3, pp.293-303.

Sudret B. & Der Kiureghian (2000) *Stochastic finite element methods and reliability: A state of the art report*, Tech. Rep. n° UCB/SEMM-2000/08, University of California, Berkley

Torquato, S. (2002) *Random heterogeneous materials: Microstructure and macroscopic properties.* Springer Verlag.

Zhang J. & Ellingwood B. (1994) Orthogonal series expansion of random fields in reliability analysis. *Journal of Engineering Mechanics*, 120, 12, pp. 2660-2677.